CO5-1 Study of Earth and Planetary Matters by Thermoluminescence

K. Ninagawa

Department of Applied Physics, Okayama University of Science

TL OF ORDINARY CHONDRITES: Induced TL (thermoluminescence), the response of a luminescent phosphor to a laboratory dose of radiation, reflects the mineralogy and structure of the phosphor, and provides valuable information on the metamorphic and thermal history of meteorites. Especially the sensitivity of the induced TL is used to determine petrologic subtype of unequilibrated ordinary chondrites [1]. Natural TL, the luminescence of a sample that has received no irradiation in the laboratory, reflects the thermal history of the meteorite in space and on Earth. Natural TL data thus provide insights into such topics as the orbits of meteoroids, the effects of shock heating, and the terrestrial history of meteorites [2]. Usually natural TL properties are applied to find paired fragments [3-5].

We have measured TLs of 216 Yamato and 136 Asuka unequilibrated ordinary chondrites [6]. This time we measured induced and natural TL properties of thirty Yamato unequilibrated ordinary chondrites (H3: 13, L3: 12, LL3: 3, L/LL3: 2) from Japanese Antarctic meteorite collection. Sampling positions of these chondrites were measured by GPS.

PAIRED FRAGMENTS: As reliable pairing approach, TL properties within large chondrites were analyzed, taking advantage of the fact that serial samples from these meteorites are known to be paired. Then a set of TL pairing criteria: 1) the natural TL peak height ratios, LT/HT, should be within 20%; 2) that ratios of raw natural TL signal (LT) to induced TL signal (TL Sensitivity) should be within 50%; 3) the TL peak temperatures should be within 20℃ and peak widths within 10℃ was proposed [3].

Above pairing criteria were applied to the 30 samples. Figure 1 shows how to search fragments satisfying the pairing criteria 1) and 2). We found 6 TL potential paired fragments. . They constructed one H3 and five L3 groups.

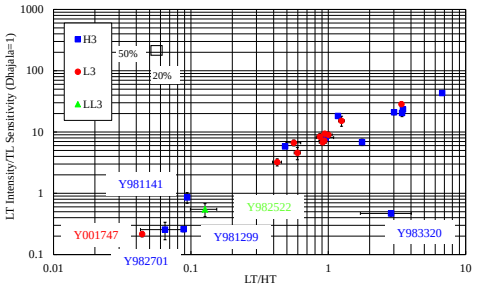

Fig.1. Ratio of LT to TL Sensitivity vs. LT/HT ratio to search fragments satisfying the pairing criteria 1) and 2).

PRIMITIVE ORDINARY CHONDRITES: Most of the chondrites had TL sensitivities over 0.1 (Dhajala=1), corresponding to petrologic subtype 3.5-3.9. Four chondrites, Y982703 (LL3), Y983367 (LL3), Y983312 (L/LL3), and Y983499 (L/LL3) were revealed to be primitive ordinary chondrites, petrologic subtype 3.0-3.1, 3.0-3.1, 3.0-3.2 and 3.1, respectively. They are not conflicted to olivine heterogeneity as shown in Fig.2. It is particularly significant in understanding the nature of primitive material in the solar system.

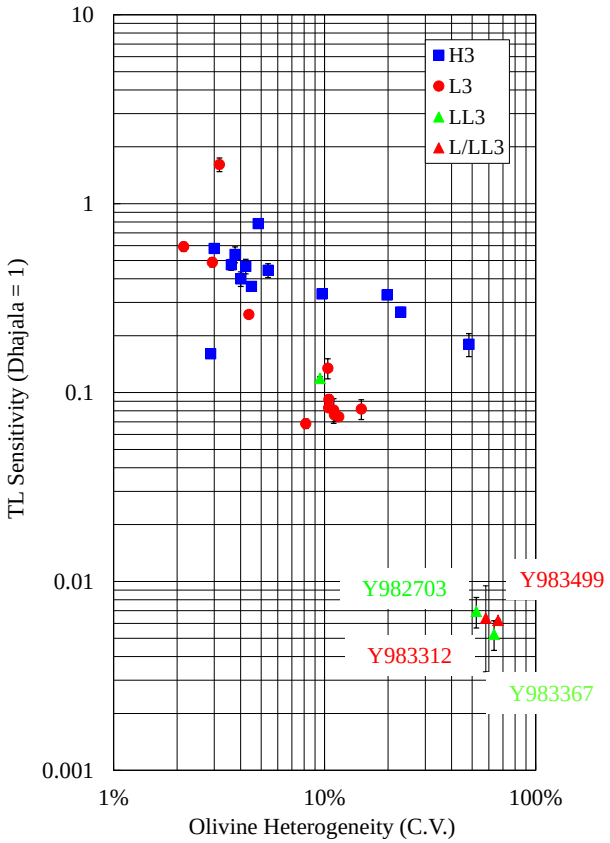

Fig.2. Dhajala-normalized TL sensitivity vs. olivine heterogeneity

REFERENCES:

[1] D. W. G. Sears *et al.*, Proceedings of Lunar and Planetary Science **21** (1991) 493-512.
[2] P. H. Benoit *et al.*, Icarus **94** (1991) 311-325.
[3] K. Ninagawa *et al.*, Antarctic Meteorite Research **11** (1998) 1-17.
[4] K. Ninagawa *et al.*, Antarctic Meteorite Research **15** (2002) 114-121.
[5] K. Ninagawa *et al.*, Antarctic Meteorite Research **18** (2005) 1-16.
[6]K. Ninagawa *et al.*, 36th Symposium on Antarctic Meteorites (NIPR, Tokyo), (2013) 56-57.

採択課題番号 25010　　熱ルミネッセンスによる地球惑星物質の研究　　一般通常

（岡山理大）蜷川清隆、西戸裕嗣

CO5-2 Characteristics of Calcite Thermoluminescence Studied for Paleoenvironmental Reconstruction of East Asia

N. Hasebe, K. Ito[1], K. and M. Ogata[1]

Institute of Nature and Environmental Technology, Kanazawa University
[1]Graduate School of Natural Science and Technology, Kanazawa University

INTRODUCTION: Luminescence dating observes the natural accumulated radiation damage caused by radioisotopes such as U and Th as the form of glow after stimulation by heating or lightening. Thermally stimulated luminescence from calcite shows strong red emission [1]. However, thermoluminescence dating of calcite is less popular because of some unknown problems; e.g., sensitivity change of calcite occurred through repeated heating of samples, possible anomalous fading, difference in characteristics of luminescence response against different kinds of radiation (e.g., gamma-ray, beta-ray, alpha-ray, and X-ray). We studied thermoluminescence characteristics of calcites focusing on their response to the various radiations, and compare it to the chemistry.

EXPERIMENTS: Calcite from Philippine, Mongol, and synthetic calcite were analyzed. Chemical composition, especially impurity concentration, was measured by LA-ICP-MS. Luminescence was detected by Photon Multiplier (R649, HAMAMATSU) with filter of 600-650 nm. First, we evaluate X-ray induced thermoluminescence property of each sample. Second, we measured luminescence caused by alpha-ray, beta-ray and gamma-ray and compare it to the luminescence induced by the X-ray. Alpha-ray source was ^{241}Am. Beta-ray source was ^{90}Sr. Gamma irradiation was carried out at the ^{60}Co gamma irradiation facility at Kyoto University Research Reactor. A known dose was given to a sample by each radiation source, and equivalent dose was estimated from the calibration line formed by x-ray irradiation. Luminescence efficiency of each radiation against x-ray (namely; a-x-value, b-x-value and c-x-value) was calculated and the relationship between luminescence characteristics and impurity concentration is examined.

RESULTS: Most calcites have thermoluminescence peak at 80 and 230 °C. In thermoluminescence peak of calcite at 80 °C, fading is detected, while 230°C peak is stable. Chemical composition of calcite shows higher concentration in Mg, P, K, Mn, Fe, Sr, and Ba (more than a few ppm). Luminescence efficiency factors (a-x-value, b-x-value and c-x-value) vary sample to sample. When compared to the chemical composition, results show negative or positive relationship between luminescence efficiency factors (a-x-value, b-x-value and c-x-value) and Mg, Mn, Fe and Sr concentrations (Fig. 1: Fe data is shown as an example). The concentration of Fe has a correlation with a luminescence emitting efficiency, while other three elements show no clear relationship to luminescence emitting efficiency. Fe plays an important role for thermoluminescence of calcite. Thermoluminescence property of calcite may be subject to multiple chemical factors (ex; Mg, Mn and Sr), therefore, further analyses on calcites with the variety of impurity are necessary to evaluate which is the principle element to control thermoluminescence properties quantitatively.

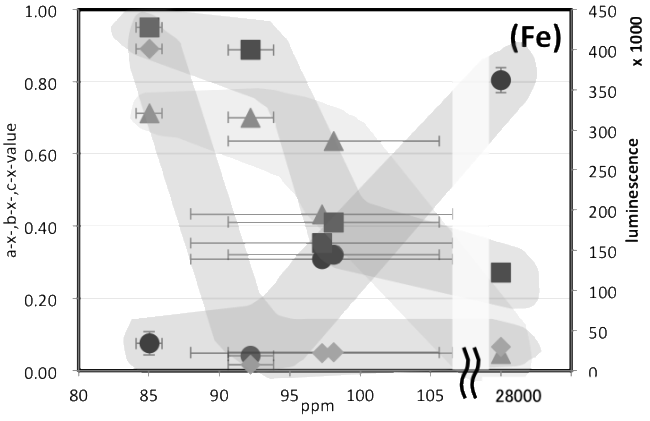

Fig. 1. Luminescence efficiency of each radiation against x-ray (namely; a-x-value for alpha-particle, b-x-value for beta-ray, and c-x-value for gamma-ray, left axis) and luminescence intensity for a constant x-ray irradiation (right axis) were plotted against Fe concentration (Horizontal axis). Circle: a-x-value. Triangle; b-x-value. Square; c-x-value. Diamond; luminescence intensity.

REFERENCES:

[1] A. Inagaki *et al.*, J. Geol. Soc. Japan 116 (2010) XIX-XX

採択課題番号 25028　　東アジアにおける古環境推定のための放射年代測定　　一般通常
（金沢大・環日本海域セ）長谷部徳子、（金沢大院・自然）伊藤健太郎、小形学

CO5-3 Atmospheric Effect of the Particles Emitted From the Burning the Waste Contaminated In Radiative Cesium

N. Ito, A. Mizohata, R. Okumura[1] and Y. Iinuma[1]

Radiation Research Center, Osaka Prefecture University,
[1]Research Reactor Institute, Kyoto University

The waste that was contaminated in radiative cesium from the Fukushima Daichi nuclear disaster is going to be cleaned or broken to smaller parts. One of some treatment for the radiative wastet is the burning . When the waste is burned, the particles are emitted from the incinerator. The indicator elements from the incinerator are thought to be sodium and potassium in fine particle. Also cesium will be the indicator of the particle from the incinerator because of the same behavior of these element as the alkali metal. We have observed the fine and coarse particles at Osaka Prefecture University at Sakai where the nearest incinerator is about 2km apart. Size distribution of potassium and cesium in the atmospheric particles are shown on Fig.1. The elements in the particles were analyzed by neutron activation analysis using KUR reactor. We use the concentration of potassium and cesium in fine particles to estimate the radio activity of radiative cesium in the particle from the incinerator that burns the waste contaminated in radiative cesium.
We show the mean concentration of potassium and cesium in coarse and fine particle at Sakai and in the soil(average in the earth) (Fig.2). To obtain the effect of the radiative particles, we have some assumptions. These are , (1)Cesium and potassium in the fine particle are almost affected from the incinerator. (2) Behavior of potassium and cesium in fine particle have the similar movement in the atmosphere. (3) Cesium in emitted particle is concentrated to 4 times after burning . From the these assumptions we can estimate the radio activity in the particle from the burning the waste contaminated in radiative cesium. We show the results in the different conditions of the radio activity of the radiative cesium in the waste (Table3). On the results maximum radio activity is 1 Bq/m3in the radiative cesium for the condition radiative cesium in 1000Bq/kg and potassiun in 1mg/kg,. This radio activity is lower than natural activity (radiative radon) and radiation dose can be estimated 7mSv/year when the maximum radio activity particle will be absorbed by breathing every time for 1 year.

Table1. Estimation of radio activity and radiation dose of the radio activity particles from the incinerator where the waste contaminated with radiative cesium(Cs) is burned. The result was estimated by the different concentration of potassium(K) in the waste on the same radio activity of radiative cesium(1000Bq/kg).

Waste	***Radiative cesium in the particle***	
K(mg/kg)	***Radio activity(Bq/m^3)***	***Radiation Dose(mSv/year)***
10000	$1x10^{-4}$	$7x10^{-6}$
1000	$1x10^{-3}$	$7x10^{-5}$
100	$1x10^{-2}$	$7x10^{-4}$
10	$1x10^{-1}$	$7x10^{-3}$
1	1	$7x10^{-2}$

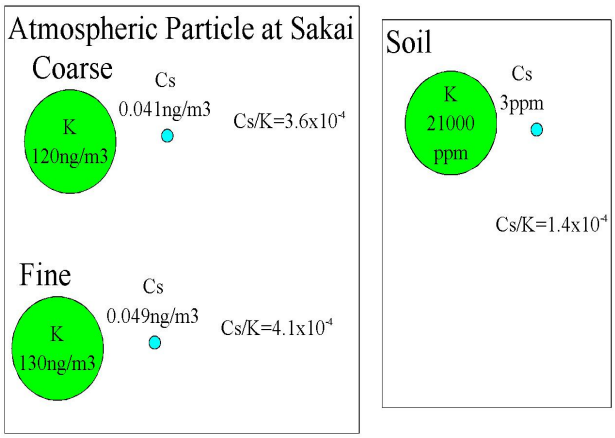

Fig.2 Mean concentrations of potassium(K) and cesium(Cs) in coarse and fine particles at Sakai. And concentrations in soil are shown.

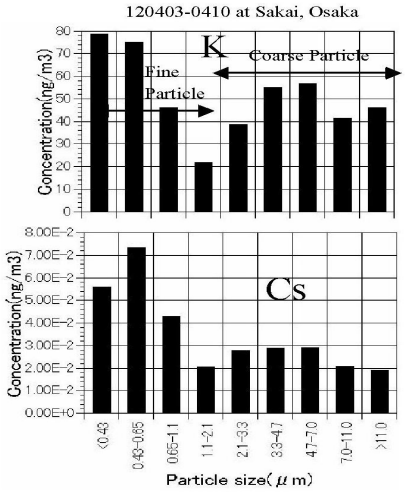

Fig.1 Size distribution of potassium(K) and cesium(Cs) in the atmospheric particles observed at Sakai, 120403-0410.

採択課題番号25029　　大気エアロゾル粒子のキャラクタリゼーション　　共同通常
（大阪府大・地域連携）伊藤憲男、溝畑 朗（京大原子炉）奥村 良、飯村勇人

CO5-4 Study on Fission Track Ages of Sedimentary Rocks in Shimanto Accretionary Complex

H. Ohira and A. Takasu

Department of Geoscience, Shimane University

INTRODUCTION: Fission track dating was applied for sedimentary rocks distributed in central part of Kii peninsula, Wakayama prefecture. The aim of this study is to estimate thermal histories of sedimentary rocks in relation with burial-uplift processes during accretion process. The Cretaceous Shimanto Belt in this area is divided into several accretionary complexes showing zonal structure. The zonal structures from north to south are composed of Hanazono, Yukawa, Miyama and Ryujin complex [1]. Previous researches revealed FT age variations across the Shimanto belt to Sambagawa metamorphic belt in the Kii region and examined the relationship between FT ages and depositional periods [2]. They concluded that samples from the Sambagawa metamorphic belts heated up to FT total stability zone (230-315 ˚C), but most samples from the Shimanto belt show no evidence heating up to such high temperature, except for one samples.

EXPERIMENTS: Samples collected from each units of the Shimanto belt were crashed and sieved and heavy minerals were concentrated by common method. Zircon and apatite were abundant in Shimanto sandstones but less amounts in the Sambagawa and Kebara Formations. Zircons were mounted in PFA Teflon, and then polished to reveal a complete internal surface. Zircons were etched in a NaOH-KOH eutectic melt at 225˚C [3] for 24-32 hours. Samples were irradiated at pneumatic tube of graphite facility (Tc-pn) of Kyoto University Reactor (KUR). After irradiation, external detectors (mica) were etched in 46% HF at 25˚C for 6-7 minutes (for mineral mounts) and for 20-50min (for NIST-SRM612). FT densities were measured at 1000× magnification with a dry objective.

RESULTS: Apparent fission track ages are obtained for Yukawa (YK-7; 133.5±6.3Ma) and Ryujin complex (RJ-7; 66.9±2.1Ma). Fission track grain age histograms comparing with depositional age of sandstone estimated by radiolarian fossils ([4], [5]) are shown in Fig. 1. The sample from Yukawa complex (YK-7) shows several age populations (90-130, 130-150 and 160Ma<). The youngest age (around 90Ma) is concordant with the younger limit of depositional age (90.4-112Ma), suggesting that the sample has not heated up to fission track annealing temperature (230-315 ˚C) during burial history. On the contrary, the youngest age component of the Ryujin complex (RJ-7; 55-60Ma) is significantly younger than the limit of depositional age (68-78Ma). This fact suggest that the sample RJ-7 buried to deeper part and heated up to temperature exceeding 300˚C, consequently fission tracks in zircon subjected to strong annealing and grain ages were thermally reset. Heating style significantly vary for each complex (geological unit). For the Ryujin complex, FT ages (69.8-67.5Ma) were reported for tuffs intercalated within sandstone [6] collected at close locality to RJ-7 (55-60Ma). The gap of FT ages (10Ma<) recognized within single complex is probably attributed to regional difference in thermal affect during burial history.

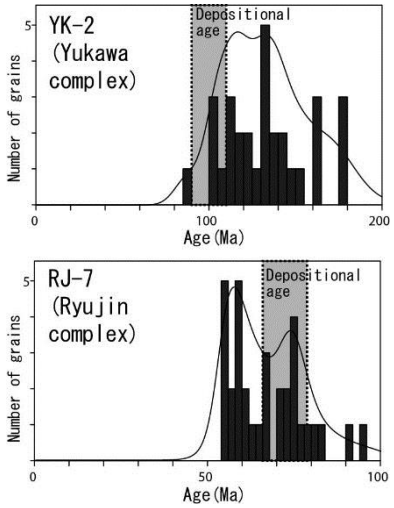

Fig.1 Fission track grain-age histograms comparing with depositional period of sandstone.

REFERENCES:

[1] H. Suzuki and S. Nakaya, The Assoc. Geological Collaboration in Japan, Monograph **59** (2012) 273-282 (in Japanese with English abstract).

[2] N. Hasebe and T. Tagami, Tectonophysics **331** (2001) 247-267.

[3] A.J.W. Gleadow *et al.*, Earth Planet. Sci. Lett. **33** (1976) 273-276.

[4]Kishu Shimanto Research Group, 2012, The Assoc. Geological Collaboration in Japan, Monograph **59** (2012) 25-34 (in Japanese with English abstract).

[5] Kishu Shimanto Research Group, The Assoc. Geological Collaboration in Japan, Monograph **59** (2012) 43-50 (in Japanese with English abstract).

[6] Kimura *et al.*, Jour. Geol. Soc. Japan, **102**, (1996) 116-124 (in Japanese with English abstract).

採択課題番号 25044 フィッション・トラック年代測定法による岩石の熱履歴解明に関する研究　一般通常
（島根大・総合理工）大平寛人、高須　晃

CO5-5 Study of Cosmogenic Nuclides by Using of Activation Analysis

Y. Tanaka, H. Ikeda1, Y. Miura1, Y. Oura
S. Sekimoto[2] and R. Okumura[2]

Graduate School of Science and Engineering, Tokyo Metropolitan University
[1]School of Science and Engineering, Faculty of Urban Liberal Arts,Tokyo Metropolitan University
[2]Research Reactor Institute, Kyoto University

I. Determination of Ultra Trace Amounts of Mn in Iron Meteorites by Preconcentration Neutron Activation Analysis

Manganes-53 is able to be found in meteorites and has largest half-life among cosmogenic radionuclides. One of practical methods for determination of ^{53}Mn is a preconcentration neutron activation analysis (preNAA) using ^{53}Mn(n, γ)^{54}Mn reaction. Content of ^{55}Mn should be required for accurate determination of ultra trace ^{53}Mn in iron meteorites by preNAA because of correction of an interference reaction, ^{55}Mn(n, 2n)^{54}Mn reaction. But accurate concentration of ^{55}Mn in iron meteorites is rarely reported. Thus we have been trying to determine a concentration of ^{55}Mn by NAA.

To avoid an interference of ^{56}Fe(n, p)^{56}Mn, preconcentration procedure for Mn from iron meteorites using only ion exchange method were developed and applied to Japan steel standard samples (JSS) and Gibeon iron meteorite last year. Although trace amount of Mn in JSS was determined successfully, a detection limit of Mn by preNAA was comparable with one by INAA using Tc-Pn due to a high procedure blank. Therefore we tried to reduce a procedure blank.

After dissolution of 0.5 g each of samples in HF, Mn was separated by cation resin exchange followed by anion exchange. Mn fraction was dropped on a filter paper, and then it was dried under infrared lump for the irradiation. The procedure was performed in a clean bench. Samples were irradiated for 4 hours at Tc-Pn in KUR.

Several determinations of procedure blanks of Mn were 12 to 28 ng. Content of Mn in blank filter papers were about 1 ng and Mn contents in acid reagents used for a chemical separation is estimated to be < 6 ng. Therefore Mn detected in procedure blank samples was supposed to be originated in the environment. It is difficult to reduce Mn content of a procedure blank than the current condition (a possible way is to simplify the procedure for Mn preconcentration). Thus the detection limit of Mn by preNAA is about 20 - 30 ng, assuming that a contribution of a procedure blank is 50%. This level is achievable by INAA using Tc-Pn. Unfortunately there is no advantage in our preNAA method at the present moment.

II. Radiochemical Measurement of Photonuclear Reaction Yields for Photon Activation Analysis.

Instrumental photon activation analysis (IPAA) meathod using (γ, n) reaction by bremsstrahlung from an electron accelerator is a complementary meathod to INAA and IPAA can determine some elements which INAA can not detemine. At the present, however, IPAA is not used well like INAA. One of reasons of a little use is guessed that it is not easy to refer reaction yield values of (γ, n) reactions for calculation of induced radioactivity. From last year we have been determining relattive reaction yields of photon nuclear reactions that is valuable for IPAA.

About 50 - 100 mg of high purity powder reagent is wrapped in aluminum foil to be formed a disk except for Ag and Au, which were foil. The disks were irradiated together with Ni monitor foils for 15 - 30 min with bremsstrahlung beam of maximun end-point energy (E_0) of 20 and/or 30 MeV from KURRI-LINAC. After irradiation, a target disks were subjected to gamma-spectrometry by a Ge detector. To reduce true coincidence effect a sample was placed far form a detector.

Target mass yields of (γ, n) reactions are shown in Fig.1 including results obtained last year. Relative yields increase smoothly with increasing target mass. Up to 80 of a target mass, reaction yields for E_0 = 20 and 30 MeV are almost consistent, though yields for E_0 = 20 MeV are systematically higher than those for 30 MeV at larger than 80 of a target mass. Several metastable products were also observed for E_0 = 30 MeV, whose yields are about 10 times smaller than the systematics. Although observed values at less than 50 of a target mass are not sufficient, the trend observed in this study can help an estimation of (γ, n) reaction yields for various elements.

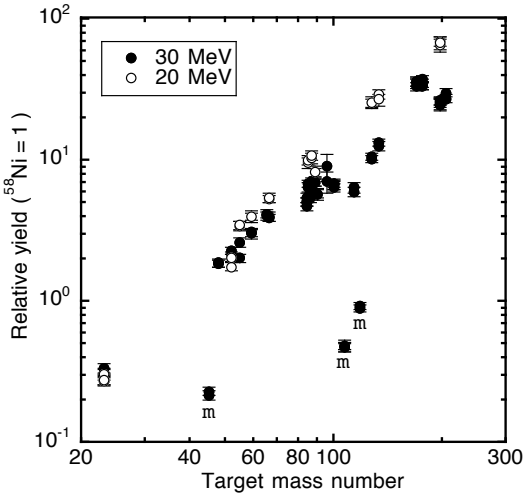

Fig. 1. Target mass yield for (γ, n) reactions at E_0 = 30 and 20 MeV. Relative yield values normalized with a yield of ^{58}Ni(γ, n)^{57}Ni are shown. Subscript "m" expresses a yield of a metastable product.

採択課題番号 25047　　放射化分析を利用した宇宙線生成核種に関する研究　　共同通常
（首都大・理工）大浦泰嗣，田中義久，池田瞳，三浦義久，白井直樹
（京大・原子炉）関本俊，奥村良

CO5-6 A Study on Redox Sensitive Elements in the Sediments at Dredged Trenches in Tokyo Bay by Instrumental Neutron Activation Analysis

T. Yamagata, K. Shozugawa, R. Okumura[1], K. Takamiya[1] and M. Matsuo

Graduate School of Arts and Sciences, The University of Tokyo
[1]Research Reactor Institute, Kyoto University

INTRODUCTION: Hypoxia is water mass with little dissolved oxygen (DO) [1]. In Tokyo Bay there are many large and deep dredged trenches, especially off the coast of Makuhari. In dredged trenches severe hypoxia has been observed in summer, and the hypoxia has disappeared in winter. But the influence of dredged trenches on hypoxia is not revealed yet. Therefore, it is important to estimate the positional and seasonal variations of hypoxia by analyzing sediments.

To estimate the sedimentary environment related to redox conditions, various elements have been used. Among them, uranium is used for the evaluation of weak reductive conditions because the redox potential of U(VI)/U(IV) is between Mn(IV)/Mn(II) and S(VI)/S(-II) [2,3]. And the method using the Th/U and Ce/U ratios was reported by Honda et al [4]. We have applied the method to evaluate the sedimentary environment in dredged trenches, which are under specific condition. In this study, sediment cores were collected from the Makuhari dredged trenches and concentrations of U, Th, and Ce in sediments were analyzed by instrumental neutron activation analysis (INAA). And then the sedimentary environment is discussed in relation to the depth profiles of Th/U and Ce/U ratios.

EXPERIMENTS: The sediment samples were collected at two dredged trenches (water depth 26.1 m and 18.9 m) and reference site (non-dredged seabed, water depth 10.6 m) off the coast of Makuhari in Tokyo Bay in August 2011. Sediments were collected by a core sampler and water quality data were also obtained.

All cores were cut in the vertical direction at 0.6-3.0 cm intervals in the laboratory, and the redox potentials of cut samples were measured. And then the samples were desalted and freeze-dried within a week.

Approximately 30 mg of sediments were packed in double polyethylene film bags to perform INAA. All samples were irradiated with neutrons at the pneumatic tube, Kyoto University Research Reactor. Two types of gamma-ray measurement were carried out corresponding to half-lives of elements. For analysis of U, samples were irradiated for 20 minutes at 1 MW or 4 minutes at 5 MW, and then gamma-ray was measured for 1200 seconds (live time) by Ge detector after 3-5 days cooling. Regarding Th and Ce, samples were irradiated for 20 minutes at 1 MW or 4 minutes at 5 MW, and the measuring time of gamma-ray was for 9000 seconds (live time) after 2-4 weeks cooling.

RESULTS: At every site surface water (< 5 m water depth) had DO less than 3 mg/L, and bottom water (> 5 m water depth) had no DO. The redox potentials of sediment samples were reductive, especially at the dredged trench (water depth 18.9 m), where most of the potentials were from -350 mV to -400 mV.

We calculated Th/U and Ce/U ratios likewise Honda et al [4], and the depth profiles of the ratios in sediment are shown in Figure. The Th/U and Ce/U ratios in the upper layers (7-8 cm from the surface) were comparatively high, and the ratios settled down to almost constant lower values below 8 cm in depth at most sites. It is known that the concentrations of Th and Ce in sediments increase when condition of seawater is oxidative [4], and the concentration of U increases when condition of seawater is reductive [4]. It is considered that the sedimentary environment of the upper layers is more oxidative than that of the lower layers. Furthermore, the ratios at the dredged trench (water depth 18.9 m) tended to be smaller than the ratios at other sites. Therefore, from Figure, it is consistent to think that the Th/U and Ce/U ratios are small at the site in which the redox potentials of sediment are reductive. And focusing on the redox potential around U(VI)/U(IV), the method using Th/U and Ce/U ratios is well reflecting the redox states in different sites.

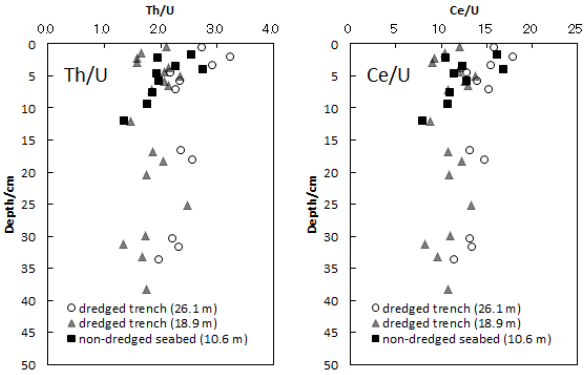

Figure. Depth profiles of Th/U (left) and Ce/U (right) ratios in the sediments collected from Tokyo Bay in August 2011.

REFERENCES:

[1] R.J. Diaz and R. Rosenberg, Science, **321** (2008) 926-929.
[2] J. Thomson, N.C. Higgs, I.W. Croudace, S. Colley and D.J. Hydes, Geochim. Cosmochim. Acta, **57** (1993) 579-595.
[3] D.R. Turner, M. Whitfield and A.G. Dickson, Geochim. Cosmochim. Acta, **45** (1981) 855-881.
[4] T. Honda and K. Kimura, Bull. Soc. Sea Water Sci., Japan, **57** (2003) 166-180 (in Japanese).

採択課題番号 25053　　汽水域および沿岸域堆積物の放射化分析　　共同通常

（東大・大学院総合）松尾基之、小豆川勝見、山形武広、堀まゆみ、添盛晃久、下元類、青木隆太朗、渡邊利奈、徐 放（京大・原子炉）高宮幸一、奥村良

CO5-7 $^{40}Ar/^{39}Ar$ Age of Volcanic Tuffs in the Eastern Africa III

H. Hyodo and T. Itaya

Research Institute of Natural Sciences,
Okayama University of Science

INTRODUCTION: A volcanic ash layer is not only a good provider for radiometric age samples, but also it represents frequency and duration of volcanic activities, which possibly affected the local and global environments. It might also act as a good preservation layer as volcanic ash might freeze biological activities at an event. Chorora Formation, Awash basin, Ethiopia in eastern Africa, attracts great interests of anthropologists since the strata bear Miocene mammalian fossils which possibly associated with the environment for the origin of hominidae. Fossils of great apes have been found in the study area. The strata consist of a number of volcanic ash layers suitable for direct radiometric dating using K-Ar system. In the previous studies [1], the K/Ar ages of the lower units ranged from 11.0 to 9.84 Ma. In order to constrain the stratigraphy for the upper units in detail, we applied $^{40}Ar/^{39}Ar$ age dating on the individual feldspar grains.

EXPERIMENTS: Experimental procedure is the same as previously described [2]. Rock samples were crushed, and sieved in #25-50 mesh. After ultrasonic cleaning in distilled water, least altered single feldspar grains were selected under microscope for high purity. The minerals were irradiated in the KUR for 24 hours at 1 MW for $^{40}Ar/^{39}Ar$ age determination. The total neutron flux was monitored by 3gr age standard [3], which was irradiated in the same sample holder. In the same batch, $CaSi_2$ and $KAlSi_3O_8$ salts were used for interfering isotope correction. The typical J-value was $(5.172 \pm 0.021) \times 10^{-3}$. In stepwise heating experiment using defocused continuous Ar ion laser beam, temperature of a mineral grain was monitored using infrared thermometer with spatial resolution of 0.3 mm and precision of 5 degrees. Extracted argon isotopes were measured using the custom made mass spectrometer [2].

RESULTS: An example of age spectra of a feldspar grain is shown in Fig. 1. The plateau age of 7.84 Ma is defined over 95% of total ^{39}Ar release, and the same ages were obtained from duplicate samples and the same stratigraphic units, indicating the consistency of the age. On the other hand, apparent ages obtained from the matrix didi not show plateau, but often exhibited increasing ages with increasing temperature. This may be caused by later alteration under a severe weathering condition in the area, and only meaningful ages seem to have been preserved in feldspars. The ages also seem to be consistent with the magnetostratigraphy in the area.

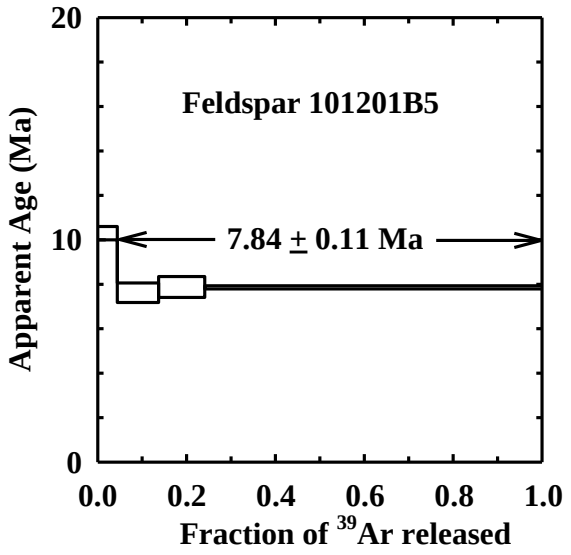

Fig. 1. $^{40}Ar/^{39}Ar$ age spectra of a feldspar from a volcanic ash strata in Ethiopia. The well defined pleateau age is obtained, and consistent results were also found in duplicates.

Recently, some mammalian fossils including great apes were found in poorly calibrated stratigraphic units, where key bed ages were unknown. In the previous age studies, some volcanic ash layers were not well calibrated as inconsistent age relations and imprecise stratigraphy were reported. The age control possibly depends on sample selection and weathering. The obtained ages provide revised stratigraphic information and may lead to a new anthropological view.

REFERENCES:

[1] D. Geraads, Z. Alemseged and H Bellon, Tertiary Research **21** Proceedings of National Academy of Science **104** (2002) 113-122.
[2] H. Hyodo, Gondwana Research **14** (2008) 609-616.
[3] J.C. Roddick, Geochim. Cosmochim. Acta **47** (1983) 887-898.

採択課題番号 25061　　東アフリカ地域火山灰の $^{40}Ar/^{39}Ar$ 年代 Ⅲ　　一般通常
（岡山理科大・自然研）兵藤博信・板谷徹丸

CO5-8 Neutron Activation Analysis of Mantle Xenolith Samples

S. Sekimoto, Y. Homura[1], N. Shirai[2], M. Ebihara[2] and T. Ohtsuki

Research Reactor Institute, Kyoto University
[1]Graduate School of Science, Kyoto University
[2] Graduate School of Science, Tokyo Metropolitan University

INTRODUCTION: For terrestrial samples, such as crustal rocks and mantle materials, accurate and reliable data of halogen abundance have been rarely reported. The contents of halogen and their relative abundance are highly informative when discussing the petrogenesis of such samples, because halogens differ in volatility from element to element. Among the halogens, especially, iodine is important element in discussion of the geochemical circulation in the earth's surface, oceanic crust, continental crust, and mantle [1]. The geochemical discussion of halogens do not promote due to the scarcity of reliable data for terrestrial rock samples.

There is a shortage of accurate and reliable data of halogens even for geological reference rocks, as can be witnessed in the data libraries, where only preferable, not certified, values and, for some rocks, no values are listed. This deficit must be largely due to the difficulty in determining trace amounts of halogens within these samples. Recently, we have improved the radiochemical neutron activation analysis (RNAA) procedure for trace amounts of halogens (Cl, Br and I), and demonstrated that our RNAA data for Br and I are more reliable and accurate than the data obtained by inductively coupled plasma mass spectrometry (ICP-MS) coupled with pyrohydrolysis preconcentration [2].

In this study, mantle xenolith samples were analyzed by our RNAA procedure. The mantle xenoliths incorporated the mantle constituents whose magma source was from >60 km of depth. We demonstrate the data for three halogens in ten mantle xenolith samples (listed in Table 1). The nine samples, other than K-10, were from south Africa, and K-10 was from Canada. The eight samples, other than K-7 and K-10, mainly consist of olivine ([Mg, Fe]$_2$SiO$_4$) and pyroxene (MgSiO$_3$), and K-7 and K-10 include garnet (Mg$_3$Al$_2$Si$_3$O$_{12}$).

Table 1: Mantle xenolith samples analyzed in this study

Sample	Major mineral	Area
K-1	Olivine, Pyroxene	Bultfontein, Kimberley
K-2	Olivine, Pyroxene	Bultfontein, Kimberley
K-3	Olivine, Pyroxene	
K-4	Olivine, Pyroxene	Monastery, Orange free state
K-5	Olivine, Pyroxene	Monastery, Orange free state
K-6	Olivine	Monastery, Orange free state
K-7	Garnet	
K-8	Olivine, Pyroxene	
K-9	Olivine, Pyroxene	
K-10	Garnet, Pyroxene	Robert victor mine

EXPERIMENTS: Trace amounts of Cl, Br and I in the 10 mantle xenolith samples were determined by RNAA. The RNAA procedure is described elsewhere [2].

RESULTS: Halogen abundances for the ten mantle xenolith samples analyzed in this study are compared in Fig. 1, where abundances are normalized to CI chondrite values [3]. Those ten samples are classified into two groups: samples including garnet (K-7 and K-10) and samples consisting of olivine and/or pyroxene. In the latter samples, absolute abundances of iodine are higher than those of chlorine and bromine within a half order of magnitude, while in K-10 chlorine abundance is highest among three halohens. Regarding K-7, the iodine abundance is higher than chlorine and bromine abundances by about two orders of magnitude. To explain this anomaly in K-7 and K-10, further studies along this line are in progress.

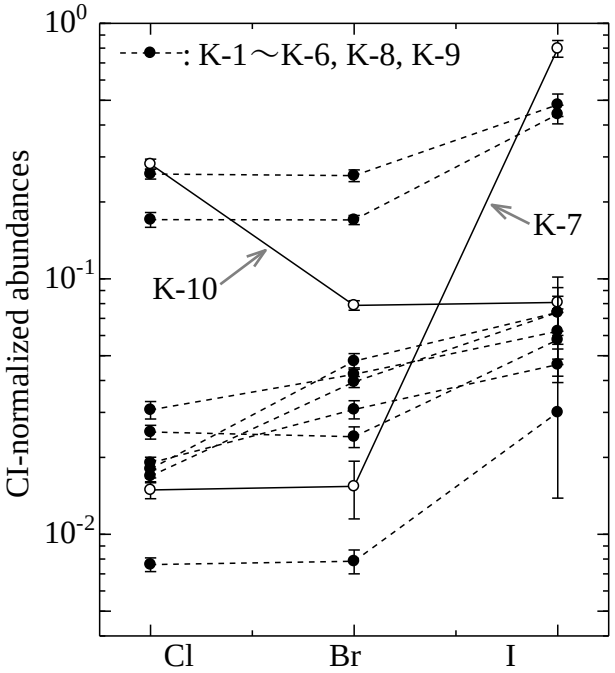

Fig. 1. Relative abundances of Cl, Br and I in mantle xenolith samples normalized to primitive meteorite values.

REFERENCES:

[1] B. Deruelle *et al.*, Earth. Planet. Sci. Lett., **108** (1992) 217-227.
[2] S. Sekimoto and M. Ebihara, Anal. Chem., **85** (2013) 6336-6341.
[3] E. Anders and N. Grevesse, Geochim. Cosmochim. Acta, 53 (1989) 197-214.

採択課題番号 25066　　京大炉（ＫＵＲ）における微小隕石及び標準岩石試料の中性子放射化分析　　共同通常

（京大・原子炉）関本　俊、奥村　良、飯沼勇人（京大院・工）布村優太
（東大院・工）石本光憲、勝村庸介、澤幡浩之、（首都大学東京・大学院・理工）海老原　充

CO5-9 Measurement of Environmental Radioactivity and Heavy Metal in Seaweed Samples in Recently

T. Ohta, T. Kubota[1], S. Fukutani[1] , T. Fujii[1] and S. Kitao[1]

Faculty of Engineering, Hokkaido University
[1] Research Reactor Institute, Kyoto University

INTRODUCTION:

Fe, Si, Zn, and Co are necessary trace elements supplied from the coastal zone to the sea. These trace elements are important for the growth and subsistence of marine organisms. In this study, we measured and compared the heavy metal content of seaweed and the $^{228}Ra/^{226}Ra$ activity ratio in seawater samples collected from Seto Island Sea, which were considered to correspond to samples from a semi-enclosed coastal sea, and the Pacific Ocean, which were considered to correspond to samples from the open sea.

EXPERIMENTS:

Eleven seaweed samples were collected from the seawater around Seto Island Sea and from the Pacific Ocean. We measured 23 elements, that is, Na, Mg, Al, Si, P, Cl, K, Ca, Ti, V, Cr, Mn, Fe, Ni, Cu, Zn, As, Br, Rb, Sr, I, Ba, and Pb, in seaweed by using XRF. We obtained Ra isotopes from the Pacific Ocean and Seto Island samples. Ra isotopes were collected on Mn-impregnated acrylic fibers and were measured by gamma-ray spectrometry. The method used for the collection of Ra isotopes from seawater has been described in detail in a previous study [1].

RESULTS:

Fig. 1 shows the concentrations of Fe, Cu, and Pb in seaweed obtained from the Pacific Ocean and from around Seto Island Sea. The concentrations of these elements in seaweed from the semi-enclosed coastal sea area tended to be higher than those in seaweed from the Pacific Ocean. In particular, the concentration of Pb in seaweed from the Seto Island samples was clearly higher. The concentrations of the major elements in the Seto Island Sea samples were the same as those in the Pacific Ocean samples. Because the major elements had a long residence time in seawater, their concentrations in seaweed were almost constant in the samples obtained from the two areas. The concentrations of the heavy elements Fe, Cu, and Pb in Kuroshio were extremely low and these elements had a short residence time; in contrast, their concentrations in seaweed from the Pacific Ocean were low. Fig. 2 shows the $^{228}Ra/^{226}Ra$ levels in the Pacific Ocean and semi-enclosed coastal sea area samples. Because the concentration of ^{226}Ra was almost 1 mBq/L in seawater, the concentration of ^{228}Ra was the same level as the $^{228}Ra/^{226}Ra$ activity ratio. Because ^{228}Ra has a short half-life of 5.8 years, the concentrations of ^{228}Ra in the Kuroshio samples were low. The concentrations of ^{228}Ra in the Seto Island samples were significantly higher than those in the Pacific Ocean samples. The ^{228}Ra and the Pb levels observed in seawater were dominant in two sources: low concentration in surface seawater from the Kuroshio and high concentration in local seawater supplied from land. The tendency seen in the ^{228}Ra concentrations in seawater would reflect those of the concentrations seen in the environment of a semi-closed system.

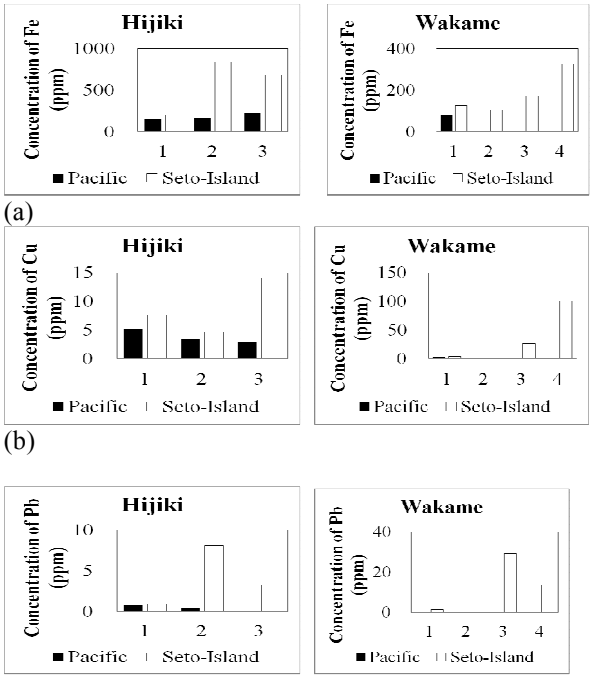

Fig. 1 Concentrations of Fe, Cu, Pb in seaweeds.
(a):Fe, (b): Cu, (c): Pb

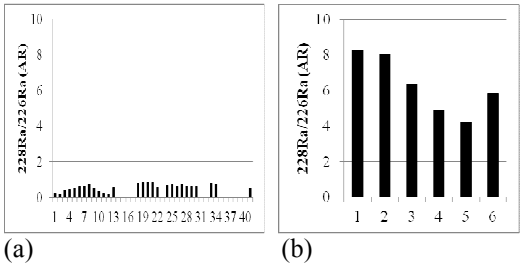

Fig. 2 $^{228}Ra/^{226}Ra$ in Pacific Ocean, Seto island.
(a) Pacific Ocean, (b) Seto Island

REFERENCES:

[1]T. Ohta *et al.*, Observation of $^{228}Ra/^{226}Ra$ activity ratio, and concentrations of ^{226}Ra and ^{228}Ra of surface seawaters in the Pacific side of Japan. Proc. Radiochimica Acta.,**1** (2011) 183-18.

採択課題番号 25070　現世から過去 100 年間の海藻中の環境放射能と重金属類の測定　　共同通常
（北大・工）太田朋子、（京大・原子炉）窪田　卓見、福谷　哲、藤井俊行、北尾真司

CO5-10 Trace Amounts of Halogens (Cl, Br and I) in 16 U.S. Geological Survey Geochemical Reference Materials

M. Ebihara and S. Sekimoto[1]

Graduate School of Science, Tokyo Metropolitan University
[1]Research Reactor Institute, Kyoto University

INTRODUCTION: Accurate and reliable data of halogen abundance have been rarely reported for terrestrial samples, such as crustal rocks and mantle materials. Since halogens differ in volatility from element to element, their content and relative abundance are highly informative when discussing the petrogenesis of such samples. Among the halogens, iodine is important element in discussion of the geochemical circulation in the earth's surface, oceanic crust, continental crust, and mantle [1]. Simply, the scarcity of reliable data for terrestrial rock samples prevents the geochemical discussion of halogens.

There is a shortage of accurate and reliable data of halogens even for geological reference rocks, as can be witnessed in the data libraries, where only preferable, not certified, values and, for some rocks, no values are listed. This deficit must be largely due to the difficulty in determining trace amounts of halogens within these samples. Recently, we have improved the radiochemical neutron activation analysis (RNAA) procedure for trace amounts of halogens (Cl, Br and I), and demonstrated that our RNAA data for Br and I are more reliable and accurate than the data obtained by inductively coupled plasma mass spectrometry (ICP-MS) coupled with pyrohydrolysis preconcentration [2].

In this study, our RNAA procedure was applied to 16 U.S. Geological Survey (USGS) geochemical reference materials (listed in Table 1), where certified values of halogens have never been reported. We will present reliable data for three halogens in 16 USGS reference materials.

Table 1: USGS geochemical reference materials analyzed in this study.

Sample	Type	Sample	Type
BHVO-2	Basalt	QLO-1a	Quartz Latite
BCR-2		COQ-1	Carbonatite
BIR-1a		CLB-1	Coal
W-2a	Diabase	SDC-1	Mica Schist
AGV-2	Andesite	Nod-P-1	Manganese - nodule
DNC-1a	Dolerite	Nod-A-1	
GSP-2	Granodiorite	SBC-1	Shale rock
DTS-2b	Dunite	SGR-1b	

EXPERIMENTS: Trace amounts of Cl, Br and I in the 16 geochemical reference materials were determined by RNAA. The RNAA procedure is described elsewhere [2]. All the samples were repeatedly analyzed two to four times.

RESULTS: Regarding BHVO-2, BCR-2, AGV-2, GSP-2, DTS-2b, QLO-1a, COQ-1, SDC-1, Nod-A-1, SBC-1, and SGR-1b, two sets of halogen data agreed within uncertainties, while in BIR-1a, W-2a, DNC-1a, CLB-1, and Nod-P-1 mean values with 1 sigma of standard deviation of four sets of halogen data obtained in this study will be reported in future work.

In CLB-1 and Nod-P-1, especially, their halogen contents are higher than those of the other reference materials by two to three orders of magnitude. Nevertheless, halogen values obtained in CLB-1 and Nod-P-1 did not always agree within uncertainties. Based on accuracy in RNAA applied in this study, homogeneity in the powder specimens may not be guaranteed for CLB-1 and Nod-P-1 and those two samples may be inadequate as a reference material.

Three halogens were also determined for two shale rocks, and it can be seen from Fig. 1 that iodine contents in shale rocks are higher than those in volcanic rocks represented by basaltic rocks (JB-1) by one to two orders of magnitude. This fact implies that iodine-enrichment can be chemical characteristics for the shale rocks, which could be important in the viewpoint of energy resources in the near future.

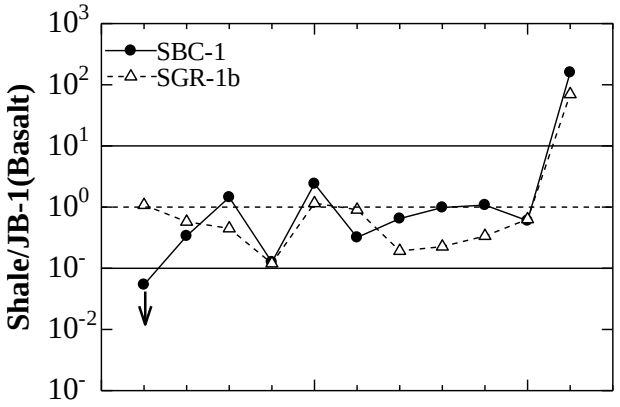

Fig.1 Ratio of elemental abundances between shale rocks and JB-1 basaltic rock.

REFERENCES:

[1] B. Deruelle *et al.*, Earth. Planet. Sci. Lett., **108** (1992) 217–227.
[2] S. Sekimoto and M. Ebihara, Anal. Chem., **85** (2013) 6336–6341.

採択課題番号 25074　　宇宙・地球化学試料中の微量ハロゲン(Cl, Br, I)の中性子放射化分析　　共同通常

（首都大学東京・大学院・理工）海老原　充（京大・原子炉）関本　俊

CO5-11 Determination of Abundance of Rare Metal Elements in Seafloor Hydrothermal Ore Deposits by INAA Techniques-3: Evaluation of Analytical Accuracy

J. Ishibashi, M. Takahashi, Y. Kimura, T. Kashimura[1], T. Yamanaka[1], R. Okumura[2] and K. Takamiya[2]

Faculty of Science, Kyushu University
[1]Graduate School of Natural Science and Technology Okayama University
[2]Research Reactor Institute, Kyoto University

INTRODUCTION: To meet recent increased demand for rare metal elements as mineral resources, high sensitive multi-element analysis becomes more important as geochemical tools for mineral exploration. Instrumental neutron activation analysis (INAA) has the advantage of non-destructive analysis and eliminates possible problems that concentrate of a specific element is often included in minerals poorly soluble during acid digestion. We have conducted preliminary studies using mineralized samples collected from active seafloor, with a view to confirm and extend the range of application of this technique. Here, we report evaluation for analyticl accuracy of INAA techniques, using reference ore materials.

EXPERIMENTS: We conducted a series of analyses of "Certified Reference Materials" which are provided by Natural Resource Canada [1]. Samples were irradiated at Pn-2 (thermal neutron flux = 5.5×10^{12} n/cm^2/sec at 1 MW) for 4 or 5 hours. The gamma ray activity was measured twice; 40 minutes measurement after 4-5 days cooling and 3 hours measurement after about 30 days cooling. Content of each nuclide was calculated by comparison of gamma ray intensities between samples and standard materials which contain known amount of Co and Cr.

RESULTS:. Analytical results of the Certified Reference Materials, CCU-1d, WMA-1a, CH-4, and DS-4 are listed in Table 1. Contents of elements are shown together with one sigma deviations for counting the pecak intensity of the gamma ray spectra. Nuclides used for the determination of elemental content are listed in the second left column with their half life in days.
The determined contents are basically agreed with the literature values (which are indicated as informational values, porvisional values, or certified values in the document provided by Natural Resource Canada). Non-negligible disagreements were found in some elements, such as Au of CCU-1d, and CH-4, and As of CH-4,. Difficulty in quantification of the gamma ray spectra due to overlap with other peaks or too high background may interfere in the determination.

REFERENCES:
[1]
http://www.nrcan.gc.ca/minerals-metals/technology/3847

Table 1 Analytical results of "Certified Reference Materials" provided by Natural Resources Canada. Units are in ppm or wt%. Numbers show contents of elements with one sigma deviations for counting the peak intensity. Numbers enclosed in parantheses are informational values, provisional values, or certified values.

element	nuclide (half life in days)	CCU-1d	WMS-1a	CH-4	DS-1
after 4-5 days cooling					
Au (ppm)	Au198 (2.69)	7.3±0.9 (14.0)	n.d. (0.3)	0.3±0.2 (0.88)	35±16 (32.5)
As (ppm)	As76 (1.09)	518±67 (545)	24.0±5.7 (30.9)	14.4±0.3 (8.8)	3000±3000 (6960)
Sb (ppm)	Sb122 (2.70)	60±13 (61.9)	7.4±2.8 (6.92)	n.d. (0.77)	96±22 (107)
Cu (wt%)	Cu64 (0.53)	22.2±4.3 (23.9)	0.14±0.1 (0.14)	n.d. (2000)	n.d. (27.1)
after 30-40 days cooling					
Se (ppm)	Se75 (119)	246±3 (244)	73±13 (87)	3.5±2.2 (2.1)	n.d. (no data)
Zn (ppm)	Zn65 (244)	24300±2600 (26300)	n.d. (130)	239±31 (200)	n.d. (206)
Fe (wt%)	Fe59 (44.4)	26.2±2.5 (29.2)	42±10 (45.4)	6.5±0.9 (5.4)	n.d. (3.0)
Ag (ppm)	Ag110m (249)	92.4±5.5 (120)	n.d. (3.7)	n.d. (2.1)	n.d. (0.47)
Sb (ppm)	Sb124 (60.2)	60.2±8.3 (61.9)	6.5±0.9 (6.92)	1.0±0.2 (0.77)	n.d. (107)

"n.d." indicates "not determined" due to too small peak intensity of the gamma ray specturm.

採択課題番号 25077　島弧火山の現世海底熱水鉱床におけるレアメタルの探索　　共同通常
（九大・理）石橋純一郎、高橋稔、木村勇気（岡大・理）柏村朋紀・山中寿朗
（京大・原子炉）奥村良、高宮幸一

CO5-12 Decontamination of Radioactive Cesium and Loss of Trace Elements in Soil

M. Yanaga, K. Sera[1], S. Goto[2], R. Okumura[3] and Y. Iinuma[3]

Graduate School of Science, Shizuoka University
[1]Cyclotron Research Center, Iwate Medical University
[2]Takizawa Institute, Japan Radioisotope Association
[3]Research Reactor Institute, Kyoto University

INTRODUCTION: A large quantity of radioisotopes was released by the Fukushima Daiichi Nuclear Power Plant accident in March 2011. The radioactive materials were released into the atmosphere and contaminated not only the air but also the ground. As a result, decontamination of radioactive materials in the soil has become a pressing issue. Especially, radioactive cesium is a problem, because soil contaminated with radioactive cesium has a long-term radiological influence due to its long half-life (30 years for ^{137}Cs). However, if contaminated soil is merely removed, the quantity of radioactive wastes will become enormous, and it will be impossible to find places to keep all the wastes. Therefore, it is very important that only radioactive cesium adhering to soil is separated, so that the quantity of radioactive waste is reduced. For this purpose, decontamination of radioactive cesium in agricultural soil was investigated by an extraction method using aqueous solutions containing potassium ions. The result of experiments on soil contaminated artificially with ^{137}Cs showed that radioactive cesium was extracted by the potassium solution, although the extraction rate decreased as the time after contamination increased [1]. However, not only radioactive cesium in soil but also essential trace elements may be removed when such decontamination methods are adopted. Therefore, in the present work, concentrations of trace elements in soil after simulated decontamination processing were determined in order to examine whether trace elements are lost or not.

EXPERIMENTS:

Preparation of samples Five grams of commercially obtained *Kuroboku* soil (andosol, a crumbly black topsoil) were placed into five centrifuge tubes. Then, 40 mL of pure water, 1M KNO_3, 1M KI, 2M KI, or 0.1 M HNO_3 were added and the mixture was stirred for one day at 25 °C. After centrifugation, each supernatant was removed. Each sample was dried after five times of washing using 40mL of pure water.

PIXE Analysis Palladium powder (Pd–carbon) has been added as an internal standard at 1 wt.% concentration. The samples were homogenized well in an agate mortar and less than 1 mg of the mixture was placed on a backing film (4 μm thick propylene film) and fixed with a 1% collodion solution. The targets were irradiated with a 2.9 MeV proton beam at Nishina Memorial Cyclotron Center, Japan Radioisotope Association, and the emitted X-rays were simultaneously measured with two Si(Li) detectors. A specially designed absorber developed for the purpose of improving sensitivity for detecting heavy elements was also used [2].

INAA The samples in polyethylene capsules were irradiated in Pn-3 for 60 seconds and for 2 hours, for short and long irradiation, respectively. The γ-ray spectroscopic measurements with an HPGe detector were performed for 120 seconds after decay time of 15 - 30 minutes for short-irradiated samples. The long -irradiated samples were measured for 4 - 24 hours after an adequate cooling time (40 - 60 days).

RESULTS: Figure 1 shows the Mn concentration in the kuroboku soil after simulated decontamination processing using various extraction solvents. As shown in this figure, the manganese concentration in the soil treated with 1 M and 2 M KI solution was lower than that in the other processed. This may indicate that not only the radioactive cesium in contaminated soil but also the essential trace elements will be removed depending on a way of extraction.

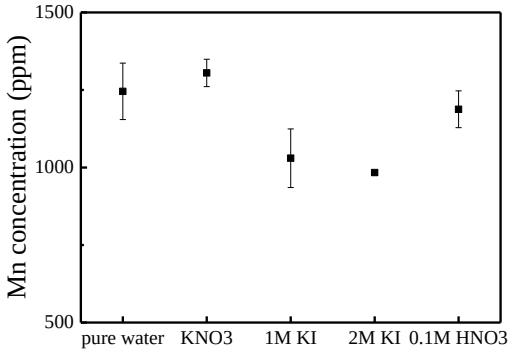

Fig. 1 Concentration of Mn in kuroboku soil after simulated decontamination processing

REFERENCES:

[1] M. Yanaga and A. Oishi, J. Radioanal. and Nucl. Chem., in press.
[2] K. Sera *et al.*, Nucl. Instr. and Meth. B, **318** (2014) 76-82.

採択課題番号 25095　除染にともなう畑土壌からの必須微量元素の損失　共同通常
（静岡大院・理）矢永誠人　（岩手医大・サイクロ）世良耕一郎　（ＲＩ協会滝沢研）後藤祥子
（京大・原子炉）奥村　良、飯村勇人

CO5-13 Neutron Activation Analysis of Iron Meteorites

N. Shirai, Y. Hidaka, S. Sekimoto[1] and M. Ebihara

Department of Chemistry, Tokyo Metropolitan University
[1]Research Reactor Institute, Kyoto University

INTRODUCTION: Iron meteorites are made of Fe-Ni metal phases with such minor minerals as schreibersite, troilite, cohenite and other Fe-Ni crubides. As most iron meteorites are believed to be sampled from the metallic core of asteroidal parent bodies, petrological, mineralogical and chemical studies of iron meteorites are fundamental for unraveling the processes of planetary differentiation. Based on phase and structure, iron meteorites were originally classified into hexadedrites, octahedrites and ataxites. The current classification is based on the chemical compositions (Ni, Ga, Ge and Ir) of iron meteorites. Chemical compositions of iron meteorites have been mostly obtained by using neutron activation analysis. In this study, a simple and effective instrumental NAA (INAA) for iron meteorites are constructed by using Kyoto University Research Reactor. Self-absorption of own gamma-rays are discussed in order to obtain data as accurately as possible. Based on the analytical data obtained, we discuss the accuracy and the precision of our data obtained by using INAA and how promisingly our analytical method can be applied to classification of iron meteorites.

EXPERIMENTS: Canyon Diablo and Cape York iron meteorites were used in this study. Iron meteorites were sawn into plate roughly 1 x 4 x 4 mm in size by using a ISOMET Low Speed Saw. Chemical standards were prepared from high-purity chemical reagents for the elements of interest. For Fe, two kinds of chemical reagents were used (Fe plate and Fe_2O_3 powder). Iron plate was cut with having similar size of iron meteorites. Nickel foil was used as standards. For other elements (Co, Cu, Ga, Ge, As, Sb, Ru, Rh, W, Re, Os, Ir, Pt and Au), standard samples were prepared by dropping known concentration solution of these elements on the three sheets of filter papers. Samples were irradiated two times with different irradiation periods at Kyoto University Research Reactor Institute (KURRI). The analytical procedure used in this study was basically similar to that described by Kong et al. [1].

RESULTS: Differences of size between samples and standards result in obtaining less accurate data due to self-absorption of their own gamma rays. The extent of self-absorption in sample depends on matrix, density, thickness and mass absorption coefficient. Iron meteorites are composed primarily of Fe-Ni metal and Fe contents of most iron meteorites are more than 90%. As ^{59}Fe emitted gamma-rays at range from low to high energy (142.65, 192.35, 1099.25 and 1291.60 keV), the extent of self-absorption of gamma-rays at the range from low to high energy can be easily examined. For these reasons, iron plate was used as simulated iron meteorites to examine the actual self-absorption of own gamma-rays. As a standard with having negligible degree of self-absorption, Fe_2O_3 powder sample was chosen. In consideration of degree of self-absorption of iron plate and Fe_2O_3 powder, differences of Fe contents in iron plate between experimental values and ideal value are due to self-absorption of own gamma-rays. In order to evaluate the degree of self-absorption of own gamma-rays, Fe contents of Fe plate samples were determined by Fe_2O_3 powder sample as standard. Iron contents calculated by using peaks at 1099.25 and 1291.60 keV were in close agreement with ideal value of iron plate, while Fe contents obtained by 142.65 and 192.35 keV peaks were 3 to 8% lower than ideal values, indicating that degree of self-absorption is significant at lower energies. In the case of analyses of iron meteorites, its Fe contents were determined by using four different gamma-ray peaks, Fe contents obtained by 142.65 and 192.35 keV peaks can be compared to those by 1099.25 and 1291.60 keV peaks to estimate the extent of self-absorption of gamma-rays at low energy. This estimated extent of self-absorption was used for the correction in determining Ge (139.53 keV), Mo (140.47 keV), Re (155.06 keV), Os (129.43 keV) and Pt (158.38 keV).

Replicate analyses of two iron meteorites (Canyon Diablo and Cape York) were carried out in order to evaluate accuracy and precision of elemental analysis. Seventeen elements could be nondestructively determined in two iron meteorites. Our values of two iron meteorites are in excellent agreement with the corresponding literature values [e.g., 2,3] within 8%. The precision of INAA experiment was defined as relative standard deviations (RSD) of replicate analyses of two iron meteorites. RSDs for most elements are less than 10 %.

The elements Ni, Ga, Ge and Ir are the most useful elements for classifying iron meteorites. Most reported Ge values of iron meteorites were determined by RNAA [4]. Both Ni and Ge abundances can be non-destructively determined by our analytical procedure with short irradiation. It is concluded that our INAA procedure is more simple and effective than analytical procedure used in previous studies [e.g., 2] for classifying the iron meteorites.

REFERENCES:

[1] P. Kong, M. Ebihara, H. Nakahara, Anal. Chem., **68** (1996) 4130-4134.
[2] J. T. Wasson and G. W. Kallemeyn, Geochim. Cosmochim Acta, 66 (2002) 2445-2473.
[2] J. T. Wasson, Geochim. Cosmochim Acta, 63 (1999) 2875-2889.
[4] D. J. Malvin, D. Wang and J. T. Wasson, Geochim. Cosmochim Acta, 48 (1984) 785-804.

採択課題番号 25097　放射化分析による宇宙・地球化学的試料の元素組成の定量　共同通常
（首都大学東京・理工）白井直樹、海老原充（京大・原子炉）関本　俊

CO5-14 Activation Analysis for Soils of Hiroshima･Nagasaki City and Gamma-ray Exposure due to Neutron-Induced Radionuclides by Atom Bomb

S. Endo, K. Shiraishi, T. Kajimoto, T. Imanaka[1], S. Fukutani[1] and T. Takatuji[2]

Graduate School of Engineering, Hiroshima University
[1] Research Reactor Institute, Kyoto University
[2]Graduate School of Fisheries Science and Environmental Studies, Nagasaki University

INTRODUCTION: For early entrance survivors in Hiroshima and Nagasaki atomic bomb (A-bomb), radiation doses from activated materials induced by the A-bomb neutrons are dominant. For estimation of such doses, element compositions of environmental materials such as soil and rubbles are necessary. Especially Sc density in soil is important for estimating radiation doses at the time of a few 10 days after explosion because ^{46}Sc has the half-life of 84 days. However, few data of Sc density in soil are available in both of Hiroshima and Nagasaki cities. Purpose of this study is evaluation of Sc density in soil and the uncertainty using activation analysis.

EXPERIMENTS: In order to compare element concentration of granite, stone wall and roof tile with that of soil, Granite, stone wall and roof tile samples were provided from atomic-bombed sample keeping in Nagasaki University.

Granite, stone wall and roof tile samples were grained to fine mesh by a mortar for activation analysis. The samples and reference rock sample of JA-1and JB-1[1] were activated in Kyoto University Reactor (KUR). Element concentrations of these samples were obtained by comparing counting rates of each identified radionuclide by Ge-detectors with those from reference rocks.

RESULTS: Twenty three element concentrations including Al, Mn, Na and Sc are obtained by the activation analysis as listed in Table 1. The obtained element concentrations for these samples are compared with values used in Dosimetry System 1986 (DS86) [2] and found roughly the same as the reported values of soil in DS86. However, a few elements show quite different composition. Especially, Na and Sc density of granite, stone wall and roof tile was roughly three times higher than those of soil. Activated nuclides of Na (^{24}Na) mainly contribute to dose from a few hours to a week after the explosion, and then Sc (^{46}Sc) becomes dominant for a few 10 days. Therefore, estimation of amount of rubble is needed for dose estimation entering the city after bombing.

REFERENCES:

[1] N. Imai *et al.* (1995) 1994 compilation of analytical data for minor and trace elements in seventeen GSJ geochemical reference samples, "igneous rock series", Geostandards Newsletter 19: 135-213.

[2] W. C. Roesch, Eds. (1986) U. S.—Japan Joint Reassessment of Atomic Bomb Radiation Dosimetry in Hiroshima and Nagasaki. Vols. 1 and 2. Radiation Effects Research Foundation.

[3] S. Endo *et al.* (2013) Neutron activation analysis for soils of Hiroshima City and Plaster under roof-tiles of Old Hiroshima House, Revisit the Hiroshima A-bomb with a Database Vol. 2, Hiroshima City 2013, ISBN: 978-4-9905935-1-3,9-14.

Table 1. Measured values of element concentration in granite, stone wall and roof tile and soil [3] comparing with Nagasaki soil in DS86 [2].

Element	Concentration（ppm）				
	Granite	stone wall	Roof tile	soil	DS86 (soil)
Ti	8000	3300	7200	5860	6320
Mg	-	13200	-	8200	7350
V	136	183	89	167	171
Al	78300	76300	86700	99600	97000
Dy	5.8	3.3	3.5	-	-
Mn	1200	960	1300	1310	1260
Na	23100	23600	13700	7890	7500
K	10500	10600	14000	7640	7540
Sm	4.9	5.6	5.0	3.9	4.0
Ce	61	63	97	43	43
Fe	97400	91400	89800	57300	58800
Th	8.7	8.9	17	7.0	7.2
Cr	389	144	177	151	152
Rb	84	84	161	70	68
Ta	3.16	3.30	5.04	0.6	0.5
Eu	4.07	2.37	1.68	1.5	1.6
Hf	6.94	5.01	6.41	6.0	6.1
Yb	7.2	5.9	7.3	-	-
Sr	719	585		134	124
Cs	5.8	2.8	10.9	4.0	4.0
Sc	84	80	79	20	20
Co	120	82	90	23	22
Zr	231	166	274	126	127

採択課題番号 25105　広島・長崎原爆中性子による誘導放射能評価のための組成分析　　共同通常
（広大院・工）遠藤　暁、白石浩太郎、梶本　剛（長大・水産・環境）高辻俊宏
（京大・原子炉）今中哲二、福谷　哲

CO5-15 Long-Term Effects of Radionuclides Originating from the Fukushima Nuclear Power Plant Accident in Airborne Particulate Matters

Y. Arai, T. Ono, K. Nakabayashi, K. Nakamachi,
S. Suzuki, Y. Okada and S. Sekimoto[1]

Graduate School of Engineering, Tokyo City University
[1]Research Reactor Institute, Kyoto University

ABSTRACT: This study is intended to elucidate the long-term effects of atmospheric radioactive cesium in Kawasaki City, Kanagawa. As a result, it became clear that the radioactive cesium activity concentration in December 2012 had decreased to about 1/105of that observed immediately after the Fukushima Daiichi nuclear power plant (FDNP) accident in March 2011 and sulfate aerosols may act as a carrier and transport radioactive cesium.

INTRODUCTION: The FDNP accident was caused by the Great East Japan Earthquake, which occurred on March 11, 2011. The artificial radionuclides ^{131}I, ^{134}Cs, and ^{137}Cs were detected in the Kanto region.

In this study, we focused on ^{131}I, ^{134}Cs, ^{137}Cs, and other radionuclides contained in airborne particulate matters (APM) sampled from filters in the Atomic Energy Research Laboratory of Tokyo City University located in the west of Kawasaki City, Kanagawa, which is about 250 km south-southwest from the FDNP.

The aim of this study was to determine the time series of the radioactive decay and the atmospheric dispersion of the artificial radionuclides by γ-ray spectrometry. Moreover, because we have been sampling the APM continuously from before the FDNP accident, we can compare the results before and after the FDNP accident.

EXPERIMENTS: After sampling the APM from the filters, we compressed the filter into an acrylic case to measure the γ-rays. A high purity germanium semiconductor detector was used for the analysis. The measurements were carried out for 80,000 s. The Seiko EG&G spectrum navigator environmental analysis program was used for nuclide analysis.

RESULTS AND DISCUSSION: Immediately after the accident at the FDNP in March 2011, ^{95}Nb, ^{97}Nb, ^{110m}Ag, ^{129}Te, ^{129m}Te, ^{131}I, ^{134}Cs, and ^{137}Cs were detected. The activity concentrations of ^{131}I, ^{134}Cs, and ^{137}Cs immediately after the accident were 1.66, 0.61, and 0.60 Bq/m^3 respectively, and the ^{131}I/^{137}Cs activity concentration ratio was 2.78. The time series of the radioactive cesium activity concentration after the FDNP accident is shown in Fig. 1. The ^{134}Cs and ^{137}Cs activity concentration in December 2012 had decreased to about 1/10^5 of the activity concentration observed immediately after the FDNP accident.

Sulfate aerosols can act as carriers of radioactive cesium. Because sulfates are formed from sulfur dioxide in the atmosphere, we indirectly examined the relationship between radioactive cesium and sulfate by comparing the activity concentration of radioactive cesium and the sulfur dioxide levels recorded by the Kawasaki pollution monitoring center. The fluctuations in the radioactive cesium concentration were similar to the fluctuation in the sulfur dioxide concentration. This finding suggests that sulfate acts as a carrier and transports radioactive cesium. As shown in Fig. 1, clear NMR resonances were found for the first time at each applied field.

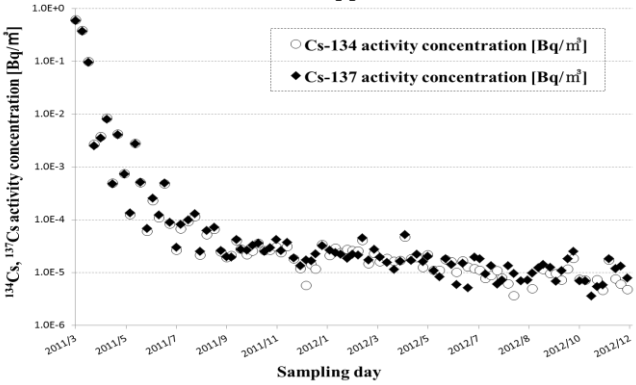

Fig. 1. Time series of ^{134}Cs and ^{137}Cs activity concentration in Kawasaki

CONCLUSION:

(1) Immediately after the accident at the FDNP in March 2011, ^{95}Nb, ^{97}Nb, ^{110m}Ag, ^{129}Te, ^{129m}Te, ^{131}I, ^{134}Cs, and ^{137}Cs were detected.

(2) The activity concentrations of ^{131}I, ^{134}Cs, and ^{137}Cs immediately after the FDNP accident were 1.66, 0.61, and 0.60 Bq/m^3, respectively, and the ^{131}I/^{137}Cs activity concentration ratio was 2.78.

(3) The ^{134}Cs and ^{137}Cs activity concentration in December 2012 had decreased to about 1/10^5 of the activity concentration observed immediately after the FDNP accident (March 2011).

(4) The fluctuation in the radioactive cesium activity concentration was similar to the fluctuations in the sulfur dioxide concentration; therefore, sulfate aerosols may act as a carrier and transport radioactive cesium.

採択課題番号 25108　　大気粒子状物質における福島原発事故由来の放射性セシウムの長期影響　　共同即時

（都市大院・工）荒井佑介、小野剛、中林和也、中町鴻、鈴木章悟、岡田往子
（京大・原子炉）関本俊

CO5-16 Volcanic and Tectonic History of Philippine Sea Plate (South of Japan) Revealed by $^{40}Ar/^{39}Ar$ Dating Technique

O. Ishizuka, T. Fujii[1], R. Okumura[1] and S. Sekimoto[1]

Geological Survey of Japan, AIST
[1]Research Reactor Institute, Kyoto University

INTRODUCTION: Submarine volcanic rocks are known to give ages different from their true eruption ages in some cases. This is due to the existence of excess ^{40}Ar in the rapidly quenched glass or Ar loss and K remobilization caused by reaction with seawater or hydrothermal fluids. Stepwise-heating analysis in $^{40}Ar/^{39}Ar$ dating is particularly useful for dating submarine volcanics.

Since this is the first time to use KUR for our laboratory, we investigated neutron flux gradient and production of interfering isotopes for $^{40}Ar/^{39}Ar$ method by irradiating standard minerals and synthetic glasses as preparation for dating of unknown samples.

EXPERIMENTS: Samples were wrapped in an aluminum foil packet and the packets were piled up in a pure aluminum (99.5% Al) irradiation capsule (9 mm diameter and 30 mm long). The irradiation capsule was partitioned into 3 compartments to minimize the uncertainty of the sample positions at irradiation. The irradiation capsule was wrapped with 0.5 mm-thick Cd-foil before irradiation. The capsule was irradiated 2 hours at 5 MW in Hyd facility of KUR. Analyses were conducted using $^{40}Ar/^{39}Ar$ geochronology facility at the Geological Survey of Japan/AIST following the analytical procedure described in [1].

RESULTS:

1) Correction for interfering isotopes

Reaction of nuclides other than ^{39}K, especially Ca, K, and Cl, with neutron produces undesirable interfering argon isotopes for $^{40}Ar/^{39}Ar$ dating. Correction factors were determined by the analysis of synthetic $KFeSiO_4$ glass and fused CaF_2 (99.9% CaF_2). Isotopic ratios of potassium-derived $^{40}Ar_K$ to $^{39}Ar_K$ and $^{38}Ar_K$ to $^{39}Ar_K$ were measured by analysis of the $KFeSiO_4$ glass following the same procedure as a sample analysis. Ratios of Ca-derived isotopes, $(^{39}Ar/^{37}Ar)_{Ca}$ and $(^{36}Ar/^{37}Ar)_{Ca}$ were determined by analysis of CaF_2.

Table 1 shows correction factors for the two different locations within a singe irradiation capsule. The factors are consistent within analytical error. This indicates that production of interference isotopes did not show significant spatial variation. The correction factors obtained here is smaller than that for obtained in JRR3 reactor (hydraulic irradiation facility), which means that thermal neutron which cause production of interfering isotopes was effectively removed by Cd-foil wrapping the irradiation capsule. This level of interference correction factors is highly suitable for $^{40}Ar/^{39}Ar$ dating.

Table 1. Interference correction factor obtained from irradiation at Hyd facility of KUR. Factors for JRR3 are also shown for comparison.

	K-derived interference		Ca-derived interference			
	$(^{38}Ar/^{39}Ar)_K$	error	$(^{39}Ar/^{37}Ar)_{Ca}$	error	$(^{36}Ar/^{37}Ar)_{Ca}$	error
KUR	0.01139	0.00005	0.000704	0.000014	0.000268	0.000005
KUR	0.01131	0.00010	0.000719	0.000009	0.000275	0.000005
JRR3	0.01839	0.00012	0.000918	0.000018	0.000414	0.000009

2) Flux monitor analysis

In $^{40}Ar/^{39}Ar$ dating, flux monitor minerals (we use Fish Canyon tuff sanidine (27. 5 Ma) are analyzed to estimate the neutron flux received by unknown samples. "J values" are calculated from the age and $^{40}Ar^*/^{39}Ar_K$ ratio of the flux monitor minerals. Most of the reactors are known to have a gradient in their neutron flux (e.g., [2]). Steep neutron flux gradient results in a significant difference in the neutron fluence between monitor minerals and unknown samples, which might cause large error in obtained ages. Fig. 1 shows variation of J value (i.e., neutron flux) with height from the bottom of the capsule) at two different column in the same capsule. The trend observed in the 2 different column is similar (J value decreasing with height), and the vertical gradient in J value is about 1.1-1.7% / cm. This is small enough to obtain ages with good accuracy, and comparable the value obtained at JMTR (1.5% / cm: [2]).

We will report dating results of samples next year.

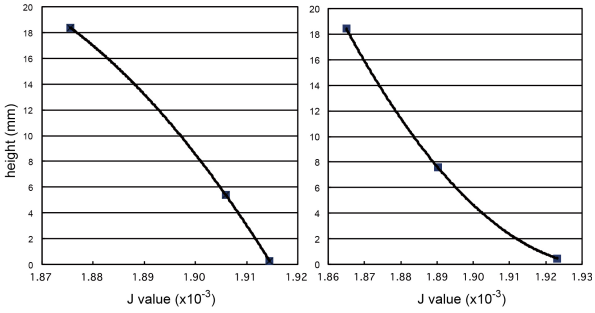

Fig. 1 J value gradient observed in a single irradiation capsule.

REFERENCES:

[1] O. Ishizuka *et al.*, Chem. Geol., **266** (2009), 274–296.
[2] O. Ishizuka, Geochem. J., **32** (1998), 243–252.

採択課題番号 25111 $^{40}Ar/^{39}Ar$ 年代測定による日本周辺海域の火山活動史及び地殻構造発達史の解明 共同通常

（産総研）石塚 治（京大・原子炉）藤井 俊行、奥村 良、関本 俊

CO5-17 Tracing Water in the Deep Earth by Ultrasensitive Halogen Analysis Using Neutron Irradiation and Noble Gas Mass Spectrometry

H. Sumino, M. Kobayashi, K. Nagao, R. Okumura[1], S. Sekimoto[1] and T. Fujii[1]

Geochemical Research Center, Graduate School of Science, University of Tokyo
[1] Research Reactor Institute, Kyoto University

INTRODUCTION: Halogens (Cl, Br, and I) are useful geochemical tracers to clarify origin of water in the mantle because they are highly incompatible and strongly partitioned into water-rich fluids and show distinctive compositions in several geochemical reservoirs in the Earth. A combination of neutron irradiation and noble gas mass spectrometry (NI-NGMS), an extension of Ar-Ar and I-Xe dating methods, allows us to simultaneously determine trace amounts of elements listed in Table 1 including halogens with naturally occurring noble gases by use of ultrahigh-sensitive noble gas mass spectrometry on neutron-irradiated samples [1,2]. This method has several advantages: (i) detection limits for halogens are three or four orders of magnitude lower than those of other conventional analytical methods, (ii) several components of different origin can be distinguished based on their relations with specific noble gas isotopes such as mantle-derived ^{3}He and by using various noble gas extraction methods such as laser microprobe, and (iii) in-situ production of radiogenic noble gas isotopes (such as ^{4}He and ^{40}Ar) after the entrapment of the noble gas component of interest in the sample can be corrected by the simultaneous determined their parent elements, such as U and K, when the age of the entrapment is known or can be assumed.

EXPERIMENTS: We carried out neutron irradiation of quartz eclogites and serpentinites from the Sanbagawa metamorphic belt, central Shikoku Island of southwestern Japan and of standard samples for NI-NGMS, Hb3gr hornblende and the Shallowater meteorite by using the hydraulic conveyer for two hours during a 5 MW operation of KUR. Noble gases in the recovered samples were extracted by heating up to 1800°C in a vacuum and analyzed with a noble gas mass spectrometer in the Radioisotope Center, the University of Tokyo [3].

Table 1. Noble gas isotopes produced by neutron irradiation*

Parent	Reaction	Noble gas product
^{6}Li	(n, α) ^{3}H (β^-)	^{3}He
^{19}F	(n, γ) β^-	^{20}Ne
$^{24, 25}$Mg	(n, α)	$^{21, 22}$Ne
^{37}Cl	(n, γ) β^-	^{38}Ar
^{39}K	(n, p)	^{39}Ar
^{40}Ca	(n, α)	^{37}Ar
$^{79, 81}$Br	(n, γ) β^-	$^{80, 82}$Kr
^{127}I	(n, γ) β^-	^{128}Xe
^{130}Ba	(n, γ) EC, EC	^{131}Xe
^{235}U	(n, fission)	^{129,131,132,134,136}Xe, ^{83,84,86}Kr

*Only important reactions in terrestrial samples are listed here.

RESULTS: Neutron flux irradiated to the samples was determined based on the amount of ^{38}Ar, ^{39}Ar and ^{128}Xe produced from ^{37}Cl, ^{39}K, and ^{127}I, respectively, in the Hb3gr and Shallowater meteorite standards. Thermal and fast neutron fluences were determined from observed ^{38}Ar/^{37}Cl and ^{39}Ar/^{39}K conversion ratios in the Hb3gr hornblende and neutron capture cross sections of corresponding reactions in Table 1. Epithermal fluence was estimated from the excess production of ^{128}Xe in the Shallowater meteorite from that calculated from the thermal neutron fluence, amount of ^{127}I in the meteorite, and ^{127}I thermal neutron capture cross section. The determined total neutron fluences in thermal, fast, and epithermal regions are $(7.9 \pm 0.1) \times 10^{21}$, $(3.20 \pm 0.03) \times 10^{21}$, and $(1.4 \pm 0.3) \times 10^{20}$ n/m^2, respectively. These fluences allow us to determine trace amounts of halogens down to: 4×10^{-10} mol of Cl, 1×10^{-10} mol of Br, and 7×10^{-14} mol of I, which are enough low to determine halogen compositions of mantle-derived rocks and minerals.
Preliminary results of halogen compositions of the quartz eclogites and serpentinites from the Sanbagawa metamorphic belt reveal that they have more than one order of magnitude higher I/Cl ratios and comparable Br/Cl ratios to those of seawater and mantle. This feature is quite similar to those of peridotites from the Sanbagawa metamorphic belt [4]. Since the metamorphic rocks had subducted into the mantle and were exhumed to the surface, the observed high I/Cl ratios possibly reflect a common feature of subducted fluids into the mantle at southwest Japan in Cretaceous. Similar enrichment only in I has been observed in deep-sea sediments and their pore water. Therefore, high I/Cl ratios ubiquitously observed in the Sanbagawa metamorphic rocks strongly suggest subduction of sediment-derived water into the mantle.

REFERENCES:

[1] G. Turner, J. Geophys. Res., **70** (1965) 5433-5445.
[2] J.K. Böhlke and J.J. Irwin, Geochim. Cosmochim. Acta, **56** (1992) 187-201.
[3] N. Ebisawa *et al.*, J. Mass Spectrom. Soc. Jpn., **52** (2004) 219-229.
[4] H. Sumino *et al.*, Earth Planet. Sci. Lett., **294** (2010) 163-172.

採択課題番号 25112　希ガス化法を用いた極微量ハロゲン測定による地球深部の水の起源の解明　　共同通常

（東大院・理・地殻化学実験施設）角野浩史、長尾敬介、小林真大
（京大・原子炉）藤井俊行、関本 俊、奥村 良

CO5-18 I-Xe Dating of Brecciated Meteorites: Elucidation of Formational Environment for Planetesimals in the Early Solar System

K. Nagao, H. Sumino, T. Fujii[1], S. Sekimoto[1] and R. Okumura[1]

Graduate School of Science, University of Tokyo
[1] Reserach Reactor Institute, Kyoto University

INTRODUCTION: An extinct nuclide ^{129}I ($T_{1/2}$ = 1.57 × 10^7 y) is known to have lived in the early stage of solar system formation. If we can determine the ratios of ^{129}I to stable isotope ^{127}I for individual meteorites, the ratios represent formation ages of the meteorites. Because ^{129}I decays to stable isotope ^{129}Xe*, an overabundance of ^{129}Xe* compared with the isotopic compositions of trapped Xe component such as Q-Xe [1] is observed in some meteorites. I-Xe dating method was developed by Jeffery and Reynolds [2], in which meteorites and an age standard meteorite are irradiated by neutrons in nuclear reactor to convert ^{127}I to ^{128}Xe*, and then ^{129}Xe*/^{128}Xe* ratios are measured for the meteorites. Time span of formation age "Δt" after formation of the standard meteorite is expressed as;

$$\Delta t = (1/\lambda)\times\ln[(^{129}Xe^*/^{128}Xe^*)_{std}/(^{129}Xe^*/^{128}Xe^*)_{sample}].$$

Brecciated meteorites record impact events occurred on their parent planetesimals, where meteoroids bombarded surface materials producing rock fragments and soils which finally solidified to rocks with brecciated structure. The impact fragmentation would have continued before and after dissipation of dense solar nebular in the early solar system. Some brecciated meteorites are known to have very high concentrations of solar He and Ne, but other brecciated ones do not contain. We measured noble gas compositions and I-Xe ages for several brecciated meteorites and found out that meteorites showing old I-Xe ages are solar gas free, but those with younger ages are enriched in solar gases. This may indicate meaningful information about timing of dissipation of solar nebula, which could be determined experimentally by I-Xe dating and noble gas analysis for brecciated meteorites [3].

EXPERIMENTS: The meteorite samples and age standard meteorite, Shallowater, weighing ca. 20 mg each were wrapped with Al-foil and inserted in an Al-capsule. The capsule was neutron irradiated in the nuclear reactor of Kyoto University. After cooling down for several months the samples were installed in a sample holder of a modified-VG3600 mass spectrometry system at the Radioisotope Center of the University of Tokyo. Noble gases were extracted by heating each sample stepwise and the extracted gases were measured with the mass spectrometer. Non-irradiated meteorites were also measured for noble gases with a modified-VG5400 noble gas mass spectrometer at the University of Tokyo.

RESULTS: Some tentative results obtained to date are shown here. The Chelyabinsk meteorite fell on 15 February 2013 in Russia as a giant fire ball. The meteorite is a breccia, showing different lithologies, numerous melt veins and dark materials produced by heavy shock heating [4]. Isotopic ratios ^{129}Xe/^{130}Xe plot against ^{128}Xe/^{130}Xe in Fig. 1 for both Chelyabinsk and Shallowater meteorites. The data points for Shallowater with 4563.3 ± 0.4 Ga absolute age [5] plot on a straight line, showing perfect closure to I-Xe system. Contrary to the Shallowater data points, those for Chelyabinsk do not show a linear trend and plot around the trapped Q-Xe [1]. The almost complete resetting of I-Xe system would have been caused by the heavy shock event occurred at 4456 ± 18 Ma proposed by Lapen et al. [6]. The Chelyabinsk meteorite does not show a presence of solar noble gases in our noble gas analyses for 12 fragments.

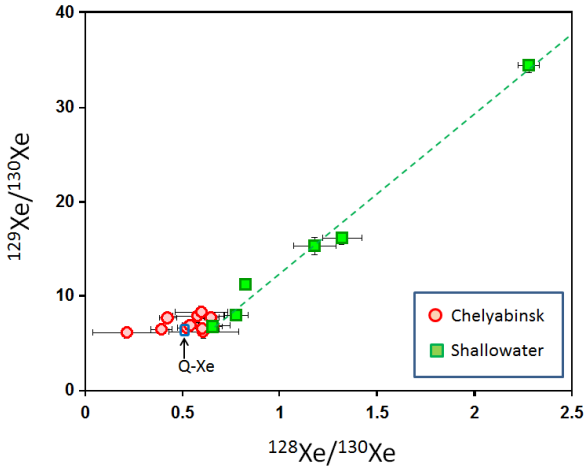

Fig. 1. Plot of ^{129}Xe/^{130}Xe vs. ^{128}Xe/^{130}Xe for Chelyabinsk and Shallowater meteorites.

REFERENCES:

[1] H. Busemann *et al.*, Meteorit. Planet. Sci., **35** (2000) 949–973.
[2] P.M. Jeffrey and J.H. Reynolds, J. Geophys. Res., **66** (1961) 3582–3583.
[3] K. Bajo, Ph.D. Thesis, Univ. Tokyo (2010).
[4] A. Bischoff *et al.*, 76th Met. Soc. (2013) Abst. #5171.
[5] J.D. Gilmour *et al.*, Meteorit. Planet. Sci., **41** (2006) 19–31.
[6] T.J. Lapen *et al.*, 45th Lunar Planet. Sci. Conf. (2014) Abst. #2561.

採択課題番号 25113　　角礫岩質隕石の I-Xe 年代測定に基づく太陽系初期の微惑星形成環境の解明　　共同通常

（東大院・理）長尾敬介、角野浩史（京大・原子炉）藤井俊之、関本俊、奥村良

CO5-19 Ar–Ar Age Determination of Petit-spot, a New Kind of Volcano

N. Hirano, H. Sumino[1], T. Fujii[2], R. Okumura[2], S. Sekimoto[2], Y. Takigami[3] and K. Nagao[1]

Center for Northeast Asian Studies, Tohoku University
[1] Geochemical Research Center, Tokyo University
[2] Research Reactor Institute, Kyoto University
[3] Kanto Gakuen University

INTRODUCTION: Tectonic plates move around on the Earth's surface with volcanic eruptions on their margins (tectonic boundaries). Undersea volcanoes erupted on an oceanic plate provide much information about the chemistry and tectonic history of the Earth. The fourth kind of volcanoes on the Earth, following three volcanic kinds which we have already known as mid-oceanic ridges, volcanic arcs and hotspots, are newly recognized on the oceanic plate off NE Japan prior to their subduction, named "petit-spot" submarine volcanoes [1]. They occur in a region of the plate, which is susceptible to fracturing due to plate subduction. The magmas produced by petit-spots originate from immediately under the plate. It is clear that the surface morphology and distribution of petit-spot volcanoes are influenced by cracks in the plate that reach the surface. The petit-spot magmas, therefore, could represent the first discovery of melting product transported directly to the surface from the deeper mantle below an old plate. The petit-spot volcanic activity, therefore, would be ubiquitous phenomenon wherever tectonic plate flexes and fractures. Recently, potential petit-spot volcanoes and lavas discovered on other areas close to the Chile Trench, Tonga Trench, around Marcus Island, and Nemuro Peninsula [2, 3]. Here, we adopt the radiometric Ar-Ar dating for the rock samples using the Kyoto University research Reactor (KUR) in order to know their eruption ages and tectonic reconstructions of eruption sites.

EXPERIMENTS: Radiometric Ar-Ar dating is commonly used to determine the ages of submarine lavas, because the traditional K-Ar dating is impossible to remove the alteration part in such rocks [4]. The rock-samples prepared for dating were crushed to 100-500 μm grains, and leached by the 1N HNO_3 at 70-60 °C for one hour. The leached samples were irradiated by neutrons in a reactor to produce ^{39}Ar from ^{39}K during a few hours. During the irradiation, samples were packed with EB-1 biotite flux monitors [5], K_2SO_4 and CaF_2 as correcting factors in an aluminum capsule. They are shielded by Cd foil in order to reduce neutron-induced ^{40}Ar from ^{40}K [6]. Then, radiogenic ^{40}Ar, daughter nuclide of radioactive ^{40}K and parent, ^{39}Ar instead of ^{40}K, were simultaneously analyzed using a mass-spectrometer with an extraction technique of multi-step heating of approximately every 100 °C between 500 to 1500 °C [7].

RESULTS: The two irradiations of samples in KUR were done on April and May, 2014. We are going to analyze the irradiated samples after cooling of samples, awaiting future analytical results. Here, we discuss previously estimating Ar-Ar ages of lavas on NW Pacific Plate, yielding eruption ages of 1.8, 4.2, 6.0, 6.5, and 8.5 Ma. The data suggest the episodic eruptions of magmas over a period involving 600 km of plate motion (approximately 10 cm per year to WNW), without any systematic spatial trend in age such that seen along oceanic island/seamount chains moving over a hotspot [8] (Fig. 1). Moreover, these volcanoes represent 8 million years of activity over a large eruption area but with low volumes of magma production.

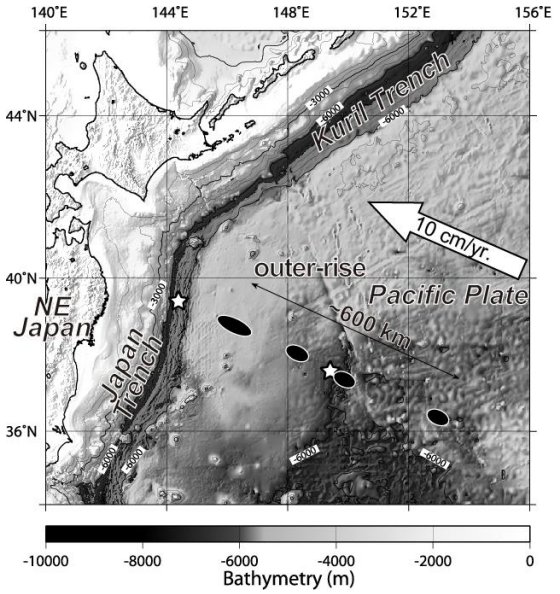

Fig. 1. Bathymetric map (contour interval, 500 m) off NE Japan. Petit-spot volcanoes are found on white stars. The estimating eruption sites are shown as black ellipses based on eruption ages and present motion of Pacific Plate (a white arrow).

REFERENCES:

[1] N. Hirano *et al.*, *Science*, **313** (2006) 1426-1428.
[2] N. Hirano *et al.*, *Geochem. J.*, **47** (2013) 249-257.
[3] N. Hirano *et al.*, *Basin Res.*, **20** (2008) 543-553.
[4] I. McDougall and T. M. Harrison, in *Geochronology and Thermochronology by the $^{40}Ar/^{39}Ar$ Method*, (Oxford, New York, 1988).
[5] N. Iwata, Ph.D. Thesis, Tokyo Univ. (1998).
[6] K. Saito, *Sci. Rep. Res. Inst. Tohoku Univ. (RITU), Japan* **A40** (1994) 185-189.
[7] N. Ebisawa *et al.*, *J. Mass Spectr. Soc. Japan*, **52** (2004), 219-229.
[8] N. Hirano *et al.*, *Geochem. J.*, **45** (2010) 157-167.

採択課題番号 25115 新種の火山のメカニズムを解明するための $^{40}Ar/^{39}Ar$ 年代測定　　共同通常
（京大・原子炉）藤井俊行、関本俊、奥村良、(関東学園大)瀧上豊、(東大院・理・地殻化学実験施設）長尾敬介、角野浩史、(東北大・東北アジア研セ）平野直人